

Heterometallic Inorganic–Organic Frameworks of Sodium–Bismuth Benzenedicarboxylates

A. Thirumurugan, Jin-Chong Tan, and Anthony K. Cheetham*

Department of Materials Science and Metallurgy, University of Cambridge, Pembroke Street, Cambridge CB2 3QZ, U.K.

Received November 9, 2009; Revised Manuscript Received December 5, 2009

ABSTRACT: Four three-dimensional (3D) inorganic–organic heterometallic Na–Bi benzenedicarboxylate (BDC) frameworks, $[\text{NaBi}(1,4\text{-BDC})_2(\text{DMF})_2]$, **1**, $[\text{NaBi}(1,4\text{-BDC})_2(\text{DMF})(\text{H}_2\text{O})]\cdot(\text{DMF})$, **2**, $[\text{NaBi}(1,3\text{-BDC})_2(\text{DMF})]$, **3**, and $[\text{NaBi}(1,3\text{-BDC})_2(\text{EtOH})]$, **4**, have been synthesized under solvothermal conditions and their structures were determined by single crystal X-ray diffraction. Compounds **1** and **2** have very similar channel structures in which infinite Na–O–Bi chains of one-dimensional inorganic connectivity are linked by the 1,4-BDC anions into 3D structures (I^1O^2). Compound **2** was obtained from **1** when it was exposed to moisture; it becomes amorphous when the solvent is removed from the channels on heating, but the activated phase has a reasonably high surface area of $71 \text{ m}^2/\text{g}$ from nitrogen porosimetry measurements. Compounds **3** and **4** are isostructural except for the solvents; they contain Na–O–Bi layers that are linked into 3D structures (P^2O^1) by 1,3-BDC anions. They are robust owing to their two-dimensional inorganic connectivity and retain their framework structures even after the removal of the solvent molecules from the channels. However, the surface area of an activated sample of **3** is only $8 \text{ m}^2/\text{g}$ due to the narrow apertures into the cavities. Tb³⁺- and Eu³⁺-doped **2** and **3** emit characteristic ligand-sensitized green and red luminescence, respectively.

Introduction

Hybrid inorganic–organic frameworks have attracted much attention in the past decade due to the growing ability to design and synthesize these novel structures for tailor-made properties and future applications.^{1–12} The main emphasis has been on gas storage and separations, for which many novel frameworks have been synthesized by the use of ligands with various shapes, sizes, and functionalities.^{13–16} Another important strategy is to create and utilize undercoordinated metal sites in the frameworks for host–guest interactions that could be harnessed for applications such as hydrogen storage.^{17–25} Recently, coordinatively flexible alkali metal ions have been employed in hybrid frameworks,^{26–29} where their oxophilicity and H₂ affinity can offer binding sites for H₂, CO₂, and other guest molecules.^{30–37} Lithium and sodium are of particular interest due to their low gravimetric density for gas storage applications.

The Bi³⁺ cation, with its geometrically flexible coordination environments, can exist with or without an active lone pair of electrons. It is well-known that in perovskites containing metal centers with ns² electrons the lone pair can play a key role in determining the collective properties such as superconductivity and ferroelectricity.^{38–41} Compounds containing Bi³⁺ cations are also used in oxidative catalysis and can act as lanthanide hosts for optical applications.^{42–44} Several bismuth carboxylates have been used as precursors for the ceramics thin-films, but very few bismuth carboxylate frameworks have been studied for porosity and related properties.^{45–48}

The III–V heterometallic zeolite analogues such as the AlPO₄ family are a unique class of compounds with a wide variety of novel structural features and applications.^{49,50} The aluminum and phosphorus cations alternate in these frame-

works. It should clearly be possible to create three-dimensional (3D) hybrid frameworks with analogous features, and this has been realized in alkali metal–lanthanide carboxylates^{51–54} and, very recently, in lithium–boron series of zeolitic imidazolate frameworks with M⁺ and M³⁺ cation ordering.^{55–57} In the present work, we describe a new family of bimetallic inorganic–organic frameworks based upon benzenedicarboxylates of Na and Bi. Compounds $[\text{NaBi}(1,4\text{-BDC})_2(\text{DMF})_2]$, **1**, $[\text{NaBi}(1,4\text{-BDC})_2(\text{DMF})(\text{H}_2\text{O})]\cdot(\text{DMF})$, **2**, $[\text{NaBi}(1,3\text{-BDC})_2(\text{DMF})]$, **3**, and $[\text{NaBi}(1,3\text{-BDC})_2(\text{EtOH})]$, **4**, have been synthesized and structurally characterized. All these compounds adopt 3D structures with one-dimensional (1D) channels. We describe their novel structural features and discuss properties such as thermal stability, porosity, and rare-earth sensitized photoluminescence.

Experimental Section

Synthesis and Characterization. Materials. Bi(NO₃)₃·5H₂O (Aldrich, 98%), Tb(NO₃)₃·5H₂O (Acros, 99.9%), Eu(NO₃)₃·5H₂O (Aldrich, 99.9%), NaOH (Fisher, 99%), 1,4-benzenedicarboxylic acid (1,4-H₂BDC) (C₈H₆O₄) (Acros, 98%), 1,3-benzenedicarboxylic acid (1,3-H₂BDC) (C₈H₆O₄) (Acros, 98%), Ethyl alcohol (EtOH) (Fisher, 99%) and dimethyl formamide (DMF) (Fisher, 99%) were used for the syntheses as purchased.

Synthesis of **1–4.** In a typical synthesis of **1**, a homogeneous mixture of Bi(NO₃)₃·5H₂O (0.1485 g, 0.3 mmol), 1,4-H₂BDC (0.2517 g, 1.5 mmol), NaOH (0.0243 g, 0.6 mmol), and DMF (6 mL), was sealed in a 23 mL stainless steel reactor with a PTFE liner and heated at 100 °C for 3 days, then cooled to room temperature. Crystals of **1** were obtained in 96% yield [based on Bi(NO₃)₃·5H₂O]. Crystals of **2** were formed from **1** over a period of few days at ambient conditions. The stability of **1** limited the number of measurements that we were able to make. Replacement of 1,4-H₂BDC by 1,3-H₂BDC in the synthesis of **1** yielded 95% [based on Bi(NO₃)₃·5H₂O] crystals of **3**. Changing the solvent from DMF to EtOH in the synthesis of **3** gave a mixture of crystals of **4** admixed with another unidentified powder phase. 2% Eu³⁺ and

*To whom correspondence should be addressed. E-mail: akc30@cam.ac.uk. Fax: +44 1223 334567.

Table 1. Crystal Data and Structure Refinement Parameters for **1** and **2**

structure parameter	1	2
empirical formula	C ₂₂ H ₂₂ N ₂ O ₁₀ NaBi	C ₂₂ H ₂₄ N ₂ O ₁₁ NaBi
formula weight	706.39	724.40
crystal system	monoclinic	monoclinic
space group	P2 ₁ /c (No. 14)	P2 ₁ /c (No. 14)
<i>a</i> / Å	7.0800(1)	7.0115(4)
<i>b</i> / Å	17.3265(4)	18.1472(9)
<i>c</i> / Å	20.8512(5)	20.1667(11)
α / °	90	90
β / °	100.004(52)	96.509(3)
γ / °	90	90
<i>V</i> / Å ³	2516.60(15)	2549.5(2)
<i>Z</i>	4	4
<i>D</i> (calc) / g cm ⁻³	1.864	1.887
μ / mm ⁻¹	7.081	6.995
total data collected	28379	26007
unique data	5755	5773
observed data [<i>I</i> > 2σ(<i>I</i>)]	4857	4467
<i>R</i> _{merg}	0.0439	0.0684
<i>R</i> indexes [<i>I</i> > 2σ(<i>I</i>)]	<i>R</i> ₁ = 0.0311 ^a <i>wR</i> ₂ = 0.0675 ^b	<i>R</i> ₁ = 0.0485 ^a <i>wR</i> ₂ = 0.1046 ^b
<i>R</i> indexes [all data]	<i>R</i> ₁ = 0.0415 ^a <i>wR</i> ₂ = 0.0711 ^b	<i>R</i> ₁ = 0.0682 ^a <i>wR</i> ₂ = 0.1152 ^b
goodness of fit (GOF)	1.078	1.035

^a $R_1 = \Sigma |F_0| - |F_c| / \Sigma |F_0|$. ^b $wR_2 = \{\Sigma [w(F_0^2 - F_c^2)^2] / \Sigma [w(F_0^2)]\}^{1/2}$. $w = 1/[o^2(F_0)^2 + (aP)^2 + bP]$, $P = [\max(F_0^2, 0) + 2(F_c^2)]/3$, where $a = 0.0210$ and $b = 9.6402$ for **1** and $a = 0.0550$ and $b = 11.1986$ for **2**.

Tb³⁺ doped **2** and **3** were prepared by using the stoichiometric amounts of Eu/Bi and Tb/Bi nitrates.

Elemental analyses of **1–3** were in good agreement with our expectations. For **1**, (C₂₂H₂₂N₂NaBiO₁₀) calcd (%): C, 37.37; H, 3.11; N, 3.96 and found (%): C, 36.89; H, 3.24; N, 3.91. For **2**, (C₂₂H₂₄N₂NaBiO₁₁) calcd (%): C, 36.44; H, 3.31; N, 3.87 and found (%): C, 36.50; H, 3.04; N, 3.74. For **3**, (C₁₉H₁₅NNaBiO₉) calcd (%): C, 36.0; H, 2.37; N, 2.21 and found (%): C, 35.69; H, 2.34 and N, 2.35. It was not possible to obtain phase pure samples of **4** for chemical analysis and other measurements.

Powder X-ray diffraction (PXRD) patterns were collected using Cu K α radiation on a Bruker D8 powder X-ray diffractometer with a position sensitive detector (LynxEye) and graphite monochromator. The program PowderCell 2.4 was used for simulation of powder patterns based upon our crystal structures. The patterns agreed well with those calculated for single-crystal structure determination. Experimental and simulated powder patterns of **1–3** are given in the Supporting Information (Figures S1–S3).

Infrared spectroscopy was performed at room temperature in the mid-IR range on a Bruker Tensor 27 infrared spectrometer equipped with an ATR diamond cell. Compounds **1–3** showed characteristic bands for the functional groups. The bands around 1550 and 1350 cm⁻¹ can be assigned to carboxylate ν_{as} C=O and ν_s C=O stretching, and the absence of a band at 1700 cm⁻¹ confirms the binding of deprotonated carboxylate groups to the cations. The band at 3435 (ν_s O-H) indicates the presence of hydroxyl groups and its ligation to the cations in **2**. Infrared spectra are given in the Supporting Information (Figures S4 and S5).

Thermogravimetric analyses (TGA) data were obtained on a TA Instruments Q500 with a heating rate of 10 °C/min in air for **2** and **3** as follows. For **2**, the first weight loss of 22.9% (calc. 22.64%) occurred around 200 °C and the second weight loss of 46.15% (calc. 45.28%) was in the 350–550 °C range. For **3**, the first weight loss of 12.17% (calc. 11.53%) occurred around 270 °C and the second weight loss of 52.26% (calc. 51.79%) was in the 350–450 °C range. In both cases, the first weight loss corresponds to the loss of DMF (**2** and **3**) and H₂O (only in **2**) molecules. The second weight loss corresponds to the loss of BDC anions. All TGA plots are given in the Supporting Information (Figures S6 and S7).

UV-visible and photoluminescence spectra on solid samples were recorded using Perkin-Elmer Lambda 750 UV/vis (Deuterium and Tungsten lamp) and LS55 fluorescence (Xenon lamp) spectrometers,

Table 2. Crystal Data and Structure Refinement Parameters for **3** and **4**

structure parameter	3	4
empirical formula	C ₁₉ H ₁₅ NNaBiO ₉	C ₁₈ H ₁₃ O ₉ NaBi
formula weight	633.29	605.25
crystal system	monoclinic	monoclinic
space group	P2 ₁ /c (No. 14)	P2 ₁ /c (No. 14)
<i>a</i> / Å	10.0214(2)	10.0681(4)
<i>b</i> / Å	12.58210(10)	12.3768(3)
<i>c</i> / Å	15.7647(2)	15.9910(7)
α / °	90	90
β / °	100.9080(10)	106.1190(18)
γ / °	90	90
<i>V</i> / Å ³	1951.86(5)	1914.32(12)
<i>Z</i>	4	4
<i>D</i> (calc) / g cm ⁻³	2.155	2.100
μ / mm ⁻¹	9.110	9.282
total data collected	28531	21060
unique data	4455	4384
observed data [<i>I</i> > 2σ(<i>I</i>)]	4094	3422
<i>R</i> _{merg}	0.0398	0.0670
<i>R</i> indexes [<i>I</i> > 2σ(<i>I</i>)]	<i>R</i> ₁ = 0.0280 ^a <i>wR</i> ₂ = 0.0650 ^b	<i>R</i> ₁ = 0.0376 ^a <i>wR</i> ₂ = 0.0699 ^b
<i>R</i> indexes [all data]	<i>R</i> ₁ = 0.0318 ^a <i>wR</i> ₂ = 0.0666 ^b	<i>R</i> ₁ = 0.0575 ^a <i>wR</i> ₂ = 0.0754 ^b
goodness of fit (GOF)	1.063	1.031

^a $R_1 = \Sigma |F_0| - |F_c| / \Sigma |F_0|$. ^b $wR_2 = \{\Sigma [w(F_0^2 - F_c^2)^2] / \Sigma [w(F_0^2)]\}^{1/2}$. $w = 1/[o^2(F_0)^2 + (aP)^2 + bP]$, $P = [\max(F_0^2, 0) + 2(F_c^2)]/3$, where $a = 0.0270$ and $b = 6.2703$ for **3** and $a = 0.0222$ and $b = 5.1803$ for **4**.

respectively. UV-visible spectra are given in the Supporting Information (Figures S8 and S9).

Single Crystal Structure Determination. Single crystal structure determination by X-ray diffraction was performed in the Kappa geometry on a Bruker-Nonius diffractometer with a Roper CCD detector, graphite monochromator and a Bruker-Nonius FR591 rotating anode X-ray source (Mo K α radiation, $\lambda = 0.71073$ Å) for **1–4**. An empirical absorption correction based on symmetry-equivalent reflections was applied using the SADABS program.⁵⁸ The structures were solved and refined using the SHELXTL PLUS suite of programs.⁵⁹ For the final refinements, the hydrogen atoms were placed geometrically and held in the riding mode. The hydrogen atoms on the water molecules were located in the difference Fourier maps, and the O–H distances were constrained to 0.85 Å. The final refinements included atomic positions for all the atoms, anisotropic thermal parameters for all the non-hydrogen atoms, and isotropic thermal parameters for the hydrogen atoms. Details of the structure solution and final refinements for the compounds are given in Tables 1 and 2.

Results and Discussion

Four 3D benzenedicarboxylates, **1–4**, have been synthesized solvothermally and characterized by X-ray diffraction and other techniques. These compounds can be categorized into two types of framework structures. Of these, compounds **1** and **2** are 1,4-benzenecarboxylates with 1D Na–O–Bi inorganic connectivity. Compounds **3** and **4** are 1,3-benzenecarboxylates with two-dimensional (2D) Na–O–Bi inorganic connectivity.

Type 1: Structures of 1,4-BDCs **1 and **2**.** The 3D 1,4-benzenedicarboxylates **1** and **2**, both containing chains of alternating BiO₈ and NaO₆ polyhedra, which are further connected to each other into a 3D structure (I' O²) with rhombic 1D channels. Though both **1** and **2** have the same framework structure, they differ in the arrangements of their solvents in the channels. The coordinating DMF molecules are projecting out into the channels from the chains in **1**. The extra coordinated water molecule in **2** replaces one of the coordinating DMF molecule in **1** and displaces them into the channels in **2**, thus creating two types of channels: one

contains coordinated DMF molecules while the other has coordinated water molecules and extra-framework DMF molecules. They also have different geometries around the Bi^{3+} cation; the coordination is hemidirected in **1** and halodirected in **2**. The finer details of these structures are described below.

The 3D 1,4-benzenedicarboxylate, $[\text{NaBi}(1,4\text{-BDC})_2\text{(DMF)}_2]$, **1**, has an asymmetric unit of 36 non-hydrogen atoms with one each of Bi^{3+} and Na^+ cations, two 1,4-benzenedicarboxylate (1,4-BDC) dianions, and two DMF molecules. The Bi^{3+} cation is eight-coordinated from eight oxygen atoms from four different BDC anions and is hemidirected with a stereochemically active lone-pair of electrons. The $\text{Bi}-\text{O}$ bond distances are in the range of 2.226(6)–2.907(4) Å. The Na^+ cation is six-coordinated by a distorted octahedron of six oxygen atoms. Among the six, four are from four different BDC anions and two are from two DMF molecules. The $\text{Na}-\text{O}$ bond distances are in the range of 2.247(5)–2.453(6) Å. The two BDC anions, BDC-1 and BDC-2, both exhibit similar coordination modes (2121)⁶⁰ with a slightly longer $\text{Bi}-\text{O}$ distance, 2.907(4) Å, involving BDC-2. The carboxyl groups in the BDC anions chelate in a bidentate manner with the Bi^{3+} cation but are monodentate with the Na^+ cation. The torsional angles between the two carboxyl groups are 14.139(8) and 43.618(6)° in BDC-1 and BDC-2, respectively. These connectivities lead to the formation of an infinite $\text{O}-\text{Na}-\text{O}-\text{Bi}-\text{O}$ 1D inorganic connectivity along the *a*-axis (Figure 1). The $\text{Na}\cdots\text{Bi}$ distances within the chains are 3.747(1) (corner sharing) and 3.459(3) Å (face sharing). The shortest $\text{Na}\cdots\text{Na}/\text{Bi}\cdots\text{Bi}$ within the chains are 7.142(4) Å along the *a*-axis. The shortest $\text{Na}\cdots\text{Na}$ and $\text{Bi}\cdots\text{Bi}$ distances between the adjacent chains are 10.334(4) and 9.957(2) along the *b*-axis and 10.348(5) and 10.364(4) Å along the *c*-axis, respectively. The structure without the DMF molecules possesses 42.3% solvent accessible void space based on a PLATON calculation.⁶¹

Compound $[\text{NaBi}(1,4\text{-BDC})_2\text{(DMF)}(\text{H}_2\text{O})]\text{(DMF)}$, **2**, has a related 3D structure ($I'\text{O}^2$) as in **1**. **2** has an extra coordinated water molecule in the asymmetric unit, which coordinates to both Bi^{3+} and Na^+ cations. The lattice DMF molecules residing in the channels having intra- and intermolecular hydrogen bonding interactions among themselves and with the projecting water molecules. The Bi^{3+} cation is eight-coordinated from seven oxygen atoms from four different BDC anions and one terminal water molecule, but unlike in **1**, here it is halodirected with a stereochemically inactive lone-pair of electrons due to the water molecule. The $\text{Bi}-\text{O}$ bond distances are in the range of 2.284(5)–2.877(6) Å. The Na^+ cation is six-coordinated with a distorted octahedron from six oxygen atoms. Among the six, four are from four different BDC anions, one is from the coordinated DMF molecule and the other is from the terminal water molecule. The $\text{Na}-\text{O}$ bond distances are in the range of 2.275(7)–2.392(6) Å. The two BDC anions in the asymmetric unit, BDC-1 and BDC-2, exhibit different coordination modes: (2121) for BDC-1 and (2120) for BDC-2. Both carboxyl groups of the BDC-1 anion chelate in a bidentate manner with one Bi^{3+} cation but are monodentate with the Na^+ cation (21), as in **1**. In BDC-2, only one of the carboxyl groups exhibits the (21) mode and the other exhibits a bidentate mode (20) through only one of the oxygen atoms. The torsional angles between the two carboxylic groups are 10.005(8) and 8.680(8)° in BDC-1 and BDC-2, respectively. These connectivities lead to the

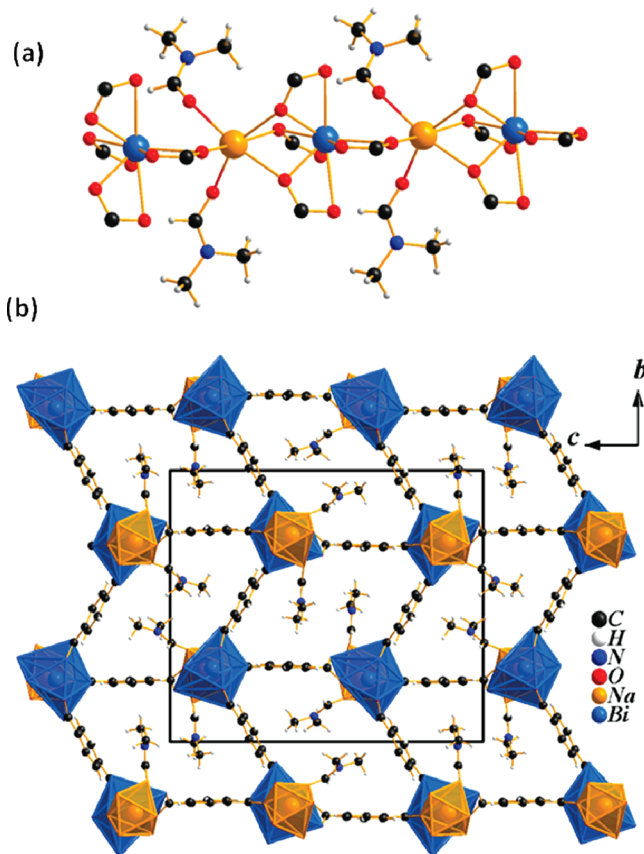


Figure 1. (a) The infinite $\text{O}-\text{Na}-\text{O}-\text{Bi}-\text{O}$ 1D inorganic connectivity along the *a*-axis and (b) the view of the 3D structure ($I'\text{O}^2$) with rhombic 1D channels down the *a*-axis in **1**.

formation of an infinite $\text{O}-\text{Na}-\text{O}-\text{Bi}-\text{O}$ 1D inorganic connectivity along the *a*-axis (Figure 2a). These chains of alternating edge and face sharing BiO_8 and NaO_6 polyhedra are further connected to four other such chains into a 3D structure ($I'\text{O}^2$) with two types of rhombic 1D channels (Figure 2b). The $\text{Na}\cdots\text{Bi}$ distances within the chains are 3.638(3) (edge sharing) and 3.471(3) Å (face sharing). The shortest $\text{Na}\cdots\text{Na}/\text{Bi}\cdots\text{Bi}$ within the chains are 7.012(2) Å along the *a*-axis. The shortest $\text{Na}\cdots\text{Na}$ and $\text{Bi}\cdots\text{Bi}$ distances between the adjacent chains are 10.169(4) and 9.743(2) along the *b*-axis and 10.110(4) and 10.092(6) Å along the *c*-axis, respectively. The structure without the water and DMF molecules possesses 44.6% of the solvent accessible void space based on a PLATON calculation.⁶¹

Type 2: Structures of 1,3-BDCs **3 and **4**.** The 3D 1,3-benzenedicarboxylates **3** and **4** both have the same perforated 2D inorganic layer based upon 10-membered sodium/bismuth rings. The layers are further connected to each other into a 3D structure ($I^2\text{O}^1$) with rhombic 1D channels. **3** and **4** have different solvent molecules in their channels. The details of these structures are described below.

The 3D 1,3-benzenedicarboxylate, $[\text{NaBi}(1,3\text{-BDC})_2\text{(DMF)}]$, **3**, has an asymmetric unit of 35 non-hydrogen atoms with one each of Bi^{3+} and Na^+ cations, two 1,3-benzenedicarboxylate (1,3-BDC) dianions, and a *N,N*-dimethylformamide (DMF) molecule. The Bi^{3+} cation is nine-coordinated from nine oxygen atoms from five different BDC anions and is halodirected with no active lone-pair of electrons. The $\text{Bi}-\text{O}$ bond distances are in the 2.332(2)–2.753(3) Å range. The Na^+ cation is six-coordinated to a

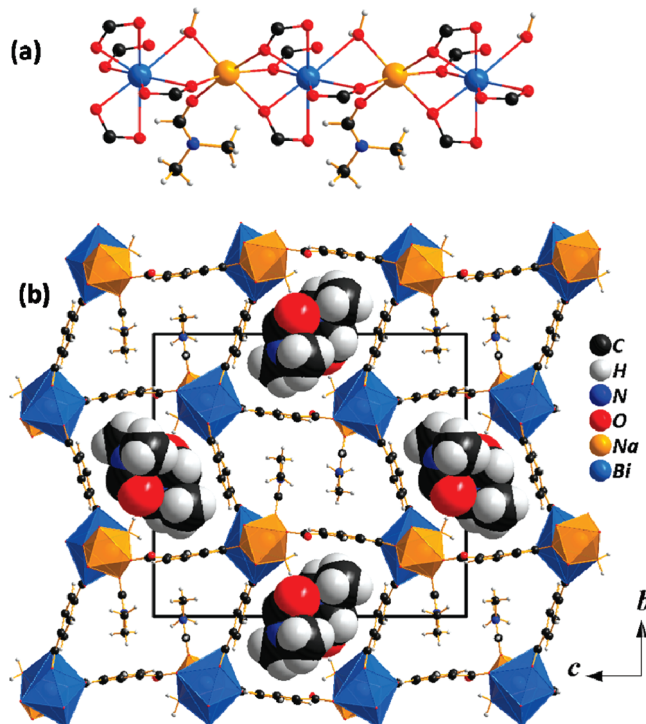


Figure 2. (a) The infinite O–Na–O–Bi–O 1D inorganic connectivity along the *a*-axis and (b) the view of the 3D structure (I^1O^2) with rhombic 1D channels down the *a*-axis in **2**.

distorted octahedron from six oxygen atoms. Among the six, five are from five different BDC anions and one is from a terminal DMF molecule. The Na–O bond distances are in the 2.258(4)–2.634(3) Å range. The two BDC anions, BDC-1 and BDC-2, exhibiting different coordination modes: (2121) for BDC-1 and (2222) for BDC-2. The carboxylic groups in the BDC-1 anion are bidentate with one Bi^{3+} cation and monodentate with one Na^+ cation to a (21) mode. Unlike in BDC-1, the two carboxyl groups of the BDC-2 anion exhibit different binding modes. Though both exhibit the (22) mode and are bidentate with one Bi^{3+} cation, in addition, one carboxyl group is monodentate with two Na^+ cations, the other monodentate with a Na^+ cation and one more Bi^{3+} cation. The torsional angles between the two carboxylic groups are 17.977(4) and 32.114(3)° in BDC-1 and BDC-2, respectively. These connectivities lead to the formation of an infinite O–Na–O–Bi–O 1D inorganic connectivity along the *b*-axis with alternative edge and face sharing. The chains connect to each other through the alternative edge shared bismuth polyhedra into an infinite O–Na–O–Bi–O 2D inorganic connectivity (I^2) perpendicular to the *a*-axis (Figure 3). These layers, which are 10.021(3) Å apart (shortest Na···Na and Bi···Bi distances between adjacent the layers), are bridged by the BDC anions into a 3D structure (I^2O^1) with rhombic 1D channels. The coordinating DMF molecules project out into these channels from the layers (Figure 4a). The Na···Bi distances within the layers are 3.892(2) (edge sharing) and 3.536(3) Å (face sharing). The shortest Na···Na and Bi···Bi within the layers are 6.481(4) and 4.389(3) Å, respectively. The structure without the DMF molecules possesses 24.6% of solvent accessible void space based on a PLATON calculation.⁶¹

The other 3D 1,3-benzenedicarboxylate, $[\text{NaBi}(1,3\text{-BDC})_2(\text{EtOH})]$, **4**, also has the same framework structure (I^2O^1), in which 2D inorganic Na–O–Bi layers (I^2) are

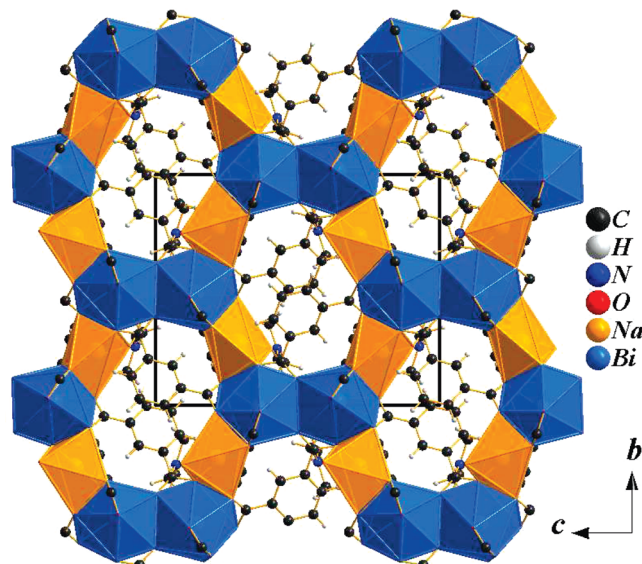


Figure 3. The infinite O–Na–O–Bi–O 2D inorganic connectivity within the *b*–*c* plane in **3**.

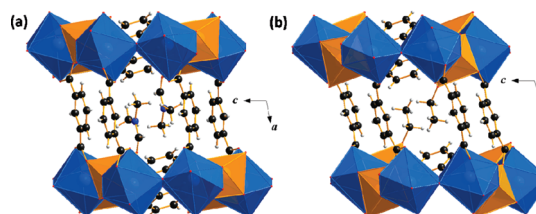


Figure 4. The view of the 3D structure (I^2O^1) with 1D channels down the *b*-axis (a) in $[\text{NaBi}(1,3\text{-BDC})_2(\text{DMF})]$, **3** and (b) in $[\text{NaBi}(1,3\text{-BDC})_2(\text{EtOH})]$, **4**.

bridged by the BDC anions as in **3**, except the terminal DMF molecule was replaced by the ethanol (EtOH) molecule (Figure 4b). It has an asymmetric unit of 29 non-hydrogen atoms. The Bi–O bond distances are in the 2.359(5)–2.782(4) Å range. The Na–O bond distances are in the 2.309(5)–2.5204(3) Å range. The torsional angles between the two carboxylic groups are 18.522(4) and 33.281(6)° in BDC-1 and BDC-2 respectively. The Na···Bi distances within the layers are 3.905(2) (edge sharing) and 3.507(2) Å (face sharing). The shortest Na···Na and Bi···Bi within the layers are 6.429(3) and 4.425(4) Å, respectively. Adjacent layers are separated by a distance of 10.068(5) Å apart (shortest Na···Na and Bi···Bi distances). The structure without the EtOH molecules possesses 21.6% of solvent accessible void space based on a PLATON calculation.⁶¹

Influence of Organic Ligands on the Inorganic Connectivity. The angle of disposition (ϑ) between the two carboxylic groups in the 1,4- and 1,3-benzenedicarboxylic acids seems to play a crucial role in the overall dimensionality as well as the inorganic connectivity of the resulting hybrid frameworks. In the present study, the 3D (I^2O^1) 1,3-benzenedicarboxylates, **3** and **4**, with (ϑ) of 120° have 2D inorganic Na–O–Bi connectivity, whereas the 3D (I^2O^1) 1,4-benzenedicarboxylates, **1** and **2** with (ϑ) of 180° have 1D inorganic Na–O–Bi connectivity. The close disposition in **3** and **4** favors the formation of 2D inorganic Na–O–Bi connectivity with a more robust framework than compounds **1** and **2**.

Porosity. Attempts were made to remove the solvent molecules from **2**, both by direct heating and by solvent exchange. These treatments always gave a poorly crystalline material, **2'**. The quantitative incorporation of one molecule of water per formula unit in **1** and the resulting formation of **2** under ambient conditions indicate the potential oxophilic interaction of the host framework with other molecules, too. Though poorly crystalline and lacking any long-range order, **2'** shows residual porosity and sorption characteristics to specific molecules. N₂ and H₂ sorption measurements at 77 K were carried out to explore the porosity and hydrogen storage behavior. At 77 K and 113 kPa, the hydrogen uptake capacity of **2'** is 0.48 wt % with a Langmuir surface area of 141.3 m²/g (Figure S10, Supporting Information). The type-1 like N₂ sorption isotherm indicates a Langmuir surface area of 71.07 m²/g and a BET surface area of 71.43 m²/g.

Unlike in **2**, the attempts to remove the solvent DMF molecules from **3** are successful by a simple thermal treatment at 270 °C. The resulting compound retains the framework structure of **3**. PXRD, CHN analysis, TGA and IR spectroscopy confirm that the resulting compound is NaBi(1,3-BDC)₂, **3'**. The framework stability can be attributed to the presence of the robust Na—O—Bi 2D inorganic connectivity in **3**. However, an N₂ sorption isotherm at 77 K gave a Langmuir surface area of only 8.28 m²/g and with type-2 nonporous behavior, though at about P/P_0 of 0.95, the adsorbed quantity of N₂ increased slightly. An H₂ sorption isotherm at 77 K (Figure S11, Supporting Information) gave a Langmuir surface area of 10.8 m²/g and with type-2 nonporous behavior, but at about the P/P_0 of 0.95, the adsorbed quantity of H₂ started increasing with a hysteresis. We speculate that this behavior could be due to the gate opening of the pores at higher pressures.

The PXRD pattern for **3'**, is shown in the Supporting Information, Figure S3. The unit cell $a = 9.83$ (1), $b = 12.73$ (2), $c = 15.53$ (1), $\beta = 94.34$ (1), and $V = 1937.78$ (3), closely resembles that of compound **3**. The absence of the DMF peaks in the IR spectra of **3'** (Supporting Information, Figure S5) and TGA data (Supporting Information, Figure S7) also suggest **3'** is a desolvated form of **3**. The lack of porosity of **3'** might be caused by a slight twisting in the benzenedicarboxylate torsional angles resulting in a smaller aperture to the channels.

Optical Properties. In order to induce multifunctional properties and investigate the sensitized luminescence,^{62,63} we have partially doped Tb and Eu (2 mol %) at the Bi site in **2** and **3**. The room temperature photoluminescence properties of all the compounds were studied using an excitation wavelength of 305 nm. The emission spectrum of the undoped compounds show a broad peak centered at ~420 nm. This emission may be attributed to intraligand luminescence, ($n \leftarrow \pi^*$) or ($\pi \leftarrow \pi^*$). A preliminary optical emission study of the doped compounds, **2a** (2 mol % Tb), **2b** (2 mol % Eu), **3a** (2 mol % Tb), and **3b** (2 mol % Eu) was carried out under UV excitation. Very efficient red and green emissions visible to the naked eye were observed for the Eu³⁺ and Tb³⁺ doped samples, respectively (inset in Figures 5 and 6). The excitation spectra have a band maximum around 305 nm, confirming that the energy transfer takes place from the ligand to the M³⁺ ion. The intersystem crossing (ISC) from the singlet to the triplet excited state of the 1,4-BDC anion occurs, followed by the energy transfer to the ⁵D₄ state of Tb³⁺ ions and to the ⁵D_j, $j = 3, 2, 1, 0$ state of Eu³⁺ ions.⁶⁴ In the Tb³⁺ doped compounds, **2a** and **3a**, the emission from the ⁵D₄

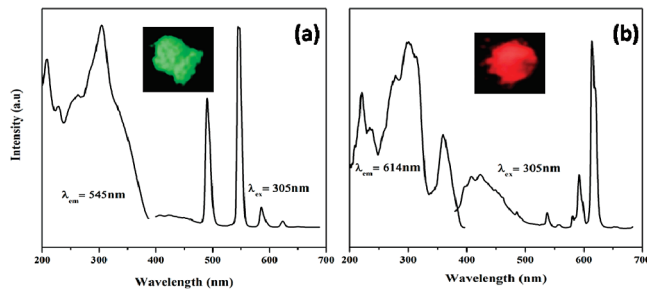


Figure 5. (a) Photoluminescence spectra of **2a** (2 mol % Tb) and (b) **2b** (2 mol % Eu). Inset shows corresponding samples under UV exposure.

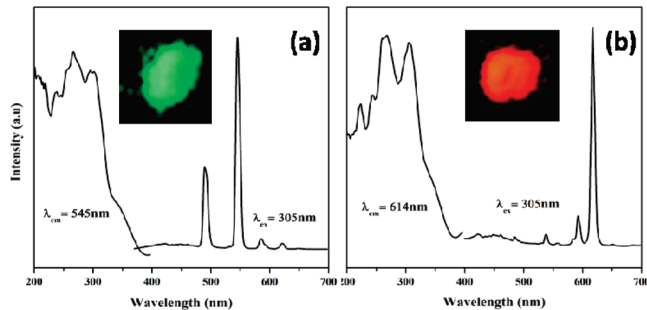


Figure 6. (a) Photoluminescence spectra of **3a** (2 mol % Tb) and (b) **3b** (2 mol % Eu). Inset shows corresponding samples under UV exposure.

⁷F_j states is responsible for the green luminescence. In Eu³⁺ doped compounds **2b** and **3b**, the emission from the ⁵D₀ → ⁷F_j states is responsible for the red luminescence. The main emission band of the intra ligand luminescence is suppressed. The intensity ratio, $I(^5D_0 \rightarrow ^7F_2)/I(^5D_0 \rightarrow ^7F_1) = R$, can be used to reveal the symmetry around the Eu³⁺ ion. The higher the symmetry, the lower is the ratio R .⁶⁵ The lower R value in **2b** compared to **3b** indicates a higher symmetry level of the coordination environment of the Eu³⁺ site in **2b**. This corroborates well with the fact that the eight coordinated metal ion (as in **2**) is more symmetric than the nine coordinated one (as in **3**). The intraligand emission at 420 nm is not quenched fully in **2b** compared with **3b**. The presence of a coordinated water molecule and its associated vibrational relaxation processes in **2b** may interfere in the quenching process and the 2D inorganic connectivity in **3b** could also play a role.

Conclusions

Four inorganic–organic heterometallic Na–Bi benzenedicarboxylates with 3D structures have been synthesized and structurally characterized. The 1,4-benzenedicarboxylates **1** and **2** have infinite Na—O—Bi chains of 1D inorganic connectivity which are linked by the 1,4-BDC anions to create 3D structures (**PO²**), whereas the 1,3-benzenedicarboxylates **3** and **4**, contain infinite Na—O—Bi layers with 2D inorganic connectivity that are linked by the 1,3-BDC anions into a 3D structure (**PO¹**). The angle of disposition (ϑ) between the two carboxylic groups in the 1,4- and 1,3-benzenedicarboxylic acids seems to play a crucial role on the overall dimensionality as well as the inorganic connectivity of the resulting hybrid frameworks. Activated **2** exhibits a reasonable level of H₂ storage capacity at 77 K, though, lacks long-range structural integrity. Compounds **3** and **4** are robust and retain their framework structures even after the removal of the solvent

molecules, probably due to their 2D inorganic connectivity. However, they exhibit very little accessible porosity. Characteristic ligand sensitized lanthanide centered luminescence is demonstrated in Tb^{3+} - and Eu^{3+} -doped derivatives of **2** and **3**.

Acknowledgment. We gratefully acknowledge the Isaac Newton Trust, Cambridge, for the financial support and the *EPSRC UK National Crystallography Service* for the single-crystal X-ray diffraction data collection. A.K.C. thanks the European Research Council for an Advanced Investigator Award. A.T. thanks Dr. Paul Saines for the help in indexing the powder XRD patterns.

Supporting Information Available: Additional plots of PXRD patterns, IR spectra, TGA, UV-vis spectra, and X-ray data files (CIF) This material is available free of charge via the Internet at <http://pubs.acs.org/>.

References

- Kitagawa, S.; Kitaura, R.; Noro, S.-i. *Angew. Chem., Int. Ed.* **2004**, *43*, 2334–2375.
- Rao, C. N. R.; Natarajan, S.; Vaidhyanathan, R. *Angew. Chem., Int. Ed.* **2004**, *43*, 1466–1496.
- Bradshaw, D.; Claridge, J. B.; Cussen, E. J.; Prior, T. J.; Rosseinsky, M. J. *Acc. Chem. Res.* **2005**, *38*, 273–282.
- Cheetham, A. K.; Rao, C. N. R.; Feller, R. K. *Chem. Commun.* **2006**, 4780–4795.
- Maspoch, D.; Ruiz-Molina, D.; Veciana, J. *Chem. Soc. Rev.* **2007**, *36*, 770–818.
- Ferry, G. *Chem. Soc. Rev.* **2008**, *37*, 191–214.
- Rao, C. N. R.; Cheetham, A. K.; Thirumurugan, A. *J. Phys.: Cond. Matt.* **2008**, 083202.
- Themed issue: Metal–organic frameworks. *Chem. Soc. Rev.* **2009**, *38*, 1201–1508.
- Ferry, G. *Dalton Trans.* **2009**, 4400–4415.
- Xiao, B.; Byrne, P. J.; Wheatley, P. S.; Wragg, D. S.; Zhao, X. B.; Fletcher, A. J.; Thomas, K. M.; Peters, L.; Evans, J. S. O.; Warren, J. E.; Zhou, W. Z.; Morris, R. E. *Nat. Chem.* **2009**, *1*, 289–294.
- Jain, P.; Ramachandran, V.; Clark, R. J.; Zhou, H. D.; Toby, B. H.; Dalal, N. S.; Kroto, H. W.; Cheetham, A. K. *J. Am. Chem. Soc.* **2009**, *131*, 13625–13627.
- Tan, J. C.; Furman, J. D.; Cheetham, A. K. *J. Am. Chem. Soc.* **2009**, *131*, 14252–14254.
- Ferry, G.; Mellot-Draznieks, C.; Serre, C.; Millange, F.; Dutour, J.; Surble, S.; Margiolaki, I. *Science* **2005**, *309*, 2040–2042.
- Banerjee, R.; Phan, A.; Wang, B.; Knobler, C.; Furukawa, H.; O’Keeffe, M.; Yaghi, O. M. *Science* **2008**, *319*, 939–943.
- Tranchemontagne, D. J.; Mendoza-Cortes, J. L.; O’Keeffe, M.; Yaghi, O. M. *Chem. Soc. Rev.* **2009**, *38*, 1257–1283.
- Natarajan, S.; Mahata, P. *Chem. Soc. Rev.* **2009**, *38*, 2304–2318.
- Forster, P. M.; Eckert, J.; Heiken, B. D.; Parise, J. B.; Yoon, J. W.; Jhung, S. H.; Chang, J.-S.; Cheetham, A. K. *J. Am. Chem. Soc.* **2006**, *128*, 16846–16850.
- Chui, S. S. Y.; Lo, S. M. F.; Charmant, J. P. H.; Orpen, A. G.; Williams, I. D. *Science* **1999**, *283*, 1148–1150.
- Kitagawa, S.; Noro, S.-i.; Nakamura, T. *Chem. Commun.* **2006**, 701–707.
- Dinca, M.; Long, J. R. *Angew. Chem., Int. Ed.* **2008**, *47*, 6766–6779.
- Chen, B.; Zhao, X.; Putkham, A.; Hong, K.; Lobkovsky, E. B.; Hurtado, E. J.; Fletcher, A. J.; Thomas, K. M. *J. Am. Chem. Soc.* **2008**, *130*, 6411–6423.
- Xi-Sen, W.; Shengqian, M.; Paul, M. F.; Daqiang, Y.; Juergen, E.; Joseph, J. L.; Brandon, J. M.; John, B. P.; Hong-Cai, Z. *Angew. Chem., Int. Ed.* **2008**, *47*, 7263–7266.
- Yong-Gon, L.; Hoi Ri, M.; Young Eun, C.; Myunghyun Paik, S. *Angew. Chem., Int. Ed.* **2008**, *47*, 7741–7745.
- Sakamoto, H.; Matsuda, R.; Bureekaew, S.; Tanaka, D.; Kitagawa, S. *Chem.—Eur. J.* **2009**, *15*, 4985–4989.
- Wang, X. S.; Ma, S.; Forster, P. M.; Yuan, D.; Eckert, J.; LÁpez, J. J.; Murphy, B. J.; Parise, J. B.; Zhou, H. C. *Angew. Chem. - Int. Ed.* **2008**, *47*, 7263–7266.
- Liu, X.; Guo, Liu, B.; Chen, W.-T.; Huang, J.-S. *Cryst. Growth Des.* **2005**, *5*, 841–843.
- Liu, Y.-Y.; Zhang, J.; Sun, L.-X.; Xu, F.; You, W.-S.; Zhao, Y. *Inorg. Chem. Commun.* **2008**, *11*, 396–399.
- Banerjee, D.; Kim, S. J.; Parise, J. B. *Cryst. Growth Des.* **2009**, *9*, 2500–2503.
- Banerjee, D.; Borkowski, L. A.; Kim, S. J.; Parise, J. B. *Cryst. Growth Des.* **2009**, *9* (11), 4922–4926.
- Lochan, R. C.; Head-Gordon, M. *Phys. Chem. Chem. Phys.* **2006**, *8*, 1357–1370.
- Férey, G.; Millange, F.; Morcrette, M.; Serre, C.; Doublet, M.-L.; Grenèche, J.-M.; Tarascon, J.-M. *Angew. Chem., Int. Ed.* **2007**, *46*, 3259–3263.
- Han, S. S.; Goddard, W. A. *J. Am. Chem. Soc.* **2007**, *129*, 8422–8423.
- Blomqvist, A.; Araújo, C. M.; Sepulchre, P.; Ahuja, R. *Proc. Natl. Acad. Sci. U. S. A.* **2007**, *104*, 20173–20176.
- Mavrandakis, A.; Tylianakis, E.; Stubos, A. K.; Froudakis, G. E. *J. Phys. Chem. C* **2008**, *112*, 7290–7294.
- Dalach, P.; Frost, H.; Snurr, R. Q.; Ellis, D. E. *J. Phys. Chem. C* **2008**, *112*, 9278–9284.
- Klontzas, E.; Mavrandakis, A.; Tylianakis, E.; Froudakis, G. E. *Nano Lett.* **2008**, *8*, 1572–1576.
- Mavrandakis, A.; Klontzas, E.; Tylianakis, E.; Froudakis, G. E. *J. Am. Chem. Soc.* **2009**, *131* (37), 13410–13414.
- Cohen, R. E. *Nature* **1992**, *358*, 136–138.
- Miles, P. A.; Kennedy, S. J.; McIntyre, G. J.; Gu, G. D.; Russell, G. J.; Koshizuka, N. *Physica C* **1998**, *294*, 275–288.
- Takahashi, Y.; Obara, R.; Nakagawa, K.; Nakano, M.; Tokita, J.-y.; Inabe, T. *Chem. Mater.* **2007**, *19*, 6312–6316.
- Bi, W.; Leblanc, N.; Mercier, N.; Auban-Senzier, P.; Pasquier, C. *Chem. Mater.* **2009**, *21*, 4099–4101.
- Postel, M.; Duñach, E. *Coord. Chem. Rev.* **1996**, *155*, 127–144.
- Neeraj, S.; Kijima, N.; Cheetham, A. K. *Chem. Phys. Lett.* **2004**, *387*, 2–6.
- Neeraj, S.; Kijima, N.; Cheetham, A. K. *Solid State Commun.* **2004**, *131*, 65–69.
- Kolitsch, U. *Acta Crystallogr. Sect. C* **2003**, *59*, m501–m504.
- Li, W.; Jin, L.; Zhu, N.; Hou, X.; Deng, F.; Sun, H. *J. Am. Chem. Soc.* **2003**, *125*, 12408–12409.
- Chen, X.; Cao, Y.; Zhang, H.; Chen, Y.; Chen, X.; Chai, X. *J. Solid State Chem.* **2008**, *181*, 1133–1140.
- Rivenet, M.; Roussel, P.; Abraham, F. *J. Solid State Chem.* **2008**, *181*, 2586–2590.
- Cheetham, A. K.; Ferry, G.; Loiseau, T. *Angew. Chem., Int. Ed.* **1999**, *38*, 3268–3292.
- Murugavel, R.; Choudhury, A.; Walawalkar, M. G.; Pothiraja, R.; Rao, C. N. R. *Chem. Rev.* **2008**, *108*, 3549–3655.
- Long, L. S.; Hu, J. Y.; Ren, Y. P.; Sun, Z. G.; Huang, R. B.; Zheng, L. S. *Main Group Metal Chem.* **2002**, *25*, 749–750.
- Canadillas-Delgado, L.; Fabelo, O.; Ruiz-Perez, C.; Delgado, F. S.; Julve, M.; Hernandez-Molina, M.; Laz, M. M.; Lorenzo-Luis, P. *Cryst. Growth Des.* **2005**, *6*, 87–93.
- Canadillas-Delgado, L.; Pasan, J.; Fabelo, O.; Hernandez-Molina, M.; Lloret, F.; Julve, M.; Ruiz-Perez, C. *Inorg. Chem.* **2006**, *45*, 10585–10594.
- Ying-Xia, Z.; Xiao-Qing, S.; Chen-Xia, D.; Ben-Lai, W.; Hong-Yun, Z. *Eur. J. Inorg. Chem.* **2008**, *2008*, 4280–4289.
- Zhang, J.; Wu, T.; Zhou, C.; Chen, S.; Feng, P.; Bu, X. *Angew. Chem., Int. Ed.* **2009**, *48*, 2542–2545.
- Wu, T.; Zhang, J.; Zhou, C.; Wang, L.; Bu, X.; Feng, P. *J. Am. Chem. Soc.* **2009**, *131*, 6111–6113.
- Wu, T.; Zhang, J.; Bu, X.; Feng, P. *Chem. Mater.* **2009**, *21*, 3830–3837.
- Sheldrick, G. M. *SADABS, Version 2007/2*; Bruker AXS Inc.: Madison, Wisconsin, 2007.
- Sheldrick, G. M. *SHELXTLPLUS Program for Crystal Structure Solution and Refinement*; University of Göttingen: Göttingen, Germany, 1997.
- For description of connectivity see: Massiot, D.; Drumel, S.; Janvier, P.; Bujoli-Doeuff, M.; Bujoli, B. *Chem. Mater.* **1997**, *9*, 6–7.
- Spek, A. L. *PLATON*; Utrecht University: Utrecht, The Netherlands, 2009.
- Bunzli, J.-C. G.; Choppin, G. R. *Lanthanide Probes in Life, Chemical and Earth Sciences. Theory and Practice*; Elsevier: Amsterdam, 1989.
- Sabbatini, N.; Guardigli, M.; Lehn, J. M. *Coord. Chem. Rev.* **1993**, *123*, 201–228.
- Blasse, G.; Grabmaier, B. C. *Luminescent Materials*; Springer: Berlin, 1994.
- Reisfeld, R.; Zigansky, E.; Gaft, M. *Mol. Phys.* **2004**, *102*, 1319–1330.